forum acusticum 2023

COMPUTING THE SOUND RADIATION OF RAILWAY TRACKS IN 2.5D USING FE COMMERCIAL CODES: APPLICATION TO TRAM TRACKS

Olivier Chiello[1*]

[1] Univ Gustave Eiffel, CEREMA, Univ Lyon, UMRAE, F-69675 Lyon, France

ABSTRACT

This paper is part of research aimed at reducing noise emissions from railway infrastructures, especially rolling noise. The track itself emits an important part of the rolling noise and the modeling of its vibro-acoustic behavior is necessary to estimate its contribution. In a first approach, the track can be considered as an infinite and invariant structure in the longitudinal direction. For the calculation of its vibratory behavior, wave-guide methods, like the Semi-Analytical Finite Element method or the Wave-guide Finite Element Method, are therefore naturally adapted. It couples a wave description in the longitudinal direction and a finite element discretization of the cross section. Concerning the sound radiation, a 2.5D approach, based on the wave decomposition of the exciting vibratory field is well adapted. The fluid medium being open, the use of boundary elements methods is most often used. However, the implementation boundary elements in 2.5D generally requires the development of dedicated codes. Alternatives exist such as infinite acoustic elements or Perfectly Match Layers which are more often implemented in commercial software. In this paper, it is shown how the sound radiation of railway tracks can be determined by combining 2D acoustic calculations and wave superposition. An application to tram tracks is proposed.

Keywords: *railway noise, tram tracks, sound radiation, wave-number domain*

Corresponding author: *olivier.chiello@univ-eiffel.fr.*

1. INTRODUCTION

In a wide range of running speeds, the main source of noise when guided vehicles pass over rails is rolling noise [1]. The track itself emits an important part of the noise and the modeling of its vibro-acoustic behavior is necessary to estimate its contribution. As a first approach, the rail is often considered as an infinite and invariant structure in the longitudinal dimension. Wave-guide methods are therefore naturally adapted to the determination of the vibrations. At low frequencies, the rail section deforms little and beam assumptions can be used. At frequencies where cross-sectional deformations appear, wave-guide finite element (WFE) or semi-analytical finite element (SAFE) methods [2, 3], which couple a wave description in the longitudinal dimension with a finite element discretization of the cross-section, are frequently used. Using this kind of approaches, track vibrations are decomposed into a finite sum of waves characterized by a wave-number and a cross-sectional deformation - a mode - which depends on the frequency.

Since the fluid medium is open, other methods are generally used for the numerical modeling of the sound radiation, in particular the boundary element method (BEM), but alternatives exist such as infinite elements or perfectly matched layers (PML), which are often implemented in commercial software. In all cases, acoustic simulations in 3D are very difficult due the extended length of track to take into account. For conventional railway tracks, the limitations of 2D radiation models have been well studied and can be heuristically corrected [4]. In contrast, studies concerning tram tracks are not frequent: the limitations of 2D models are not assessed and it seems prudent to perform 3D simulations. In ref. [2], Nilsson *et al* propose a wave-number decomposition in order to compute the sound radiated by tram tracks from several 2D simulations. However, the method is based on an in-house implementation of the BEM for computing the rail

sound radiation in the wave-number domain. Generally speaking, the use of spatial Fourier transforms to solve infinite-dimensional vibro-acoustic problems is a widely-used approach, for example in the investigation of environmental ground vibrations [5].

The method proposed in this paper is very similar to the work of Nilsson *et al* [2] excepted that 2D simulations are performed by using finite acoustic elements combined with perfectly matched layers instead of boundary elements. Furthermore, it is shown how the use of a commercial acoustic software can be used for this purpose. The trick lies in the modification of the prescribed sound speed in order to simulate the acoustic field corresponding to different structural wave-numbers. Compared with full 3D models, the main advantage of the method is that the "infinite" integration along the longitudinal dimension of the track, which makes 3D simulation extremely costly in terms of computing time, is replaced by a "finite" integration over the wave-numbers. The number of 2D simulations required can be significant, especially when some structural waves have low longitudinal attenuation, but it is shown how this can be controlled by a judicious choice of the discrete wave-numbers. An application to realistic tram tracks is then proposed, showing the potential of the proposed method.

2. DESCRIPTION OF THE METHOD

The railway track is modeled by a linear elastic structure, infinite and invariant along its length. A reference frame (x, y, z) is defined such that the coordinate x refers to the longitudinal axis of the track and coordinates (y, z) refer to the plane of its section. The objective is to determine the radiated noise resulting from the track vibratory response to a harmonic point excitation at pulsation ω. Equations are derived in the frequency domain by using a complex formalism. The method needs no further assumptions.

2.1 Track vibration

2.1.1 Spatial domain

Given the above assumptions, the vibratory response to an excitation field $\delta(x)f(y, z)$ applied to the abscissa $x = 0$ on the track can be expressed using a superposition of N waves i characterized by sectional shapes $\mathbf{v_i}(y, z)$ and

complex spatial wave-numbers $\hat{\kappa}_i$ varying with frequency:

$$\mathbf{v}(x, y, z) = \sum_{i=1}^{N} \mathbf{v_i}(y, z) e^{-j\hat{\kappa}_i |x|} \tag{1}$$

This expression is general and independent of the modeling level of the track section. For instance, in the case of analytical models based on a vertical or lateral bending beam for representing the rail, only two waves with undeformed cross-sectional shape are obtained. When the deformation of the rail section is taken into account, for instant by using SAFE or WFE models, a larger number of waves may be determined and kept.

2.1.2 Wave-number domain

The track vibratory response can be expressed in the wave-number domain using a spatial Fourier transform:

$$\begin{aligned} \tilde{\mathbf{v}}(\kappa, y, z) &= \int_{-\infty}^{+\infty} \mathbf{v}(x, y, z) e^{-j\kappa x} dx \\ &= \sum_{i=1}^{N} \mathbf{v_i}(y, z) \int_{-\infty}^{+\infty} e^{-j\hat{\kappa}_i |x|} e^{-j\kappa x} dx \\ &= \sum_{i=1}^{N} \mathbf{v_i}(y, z) \frac{2j\hat{\kappa}_i}{\kappa^2 - \hat{\kappa}_i^2} \end{aligned} \tag{2}$$

where "resonances" may occur at the complex poles corresponding to wave-numbers $\hat{\kappa}_i$, with a magnitude depending on the excitation but also on the imaginary part of the pole which is related to the longitudinal attenuation of the wave.

2.2 Track sound radiation

2.2.1 Spatial domain

The pressure $p(x, y, z)$ radiated by the track verifies the Helmholtz equation in unbounded acoustic space:

$$\begin{aligned} \Delta p + k^2 p &= 0 \\ \text{with} \quad \frac{\partial p}{\partial \mathbf{n}} &= j\omega \rho v_n \quad \text{on } S \end{aligned} \tag{3}$$

where Δ refers to the spatial Laplacian, $k = \frac{\omega}{c}$ represents the acoustic wave-number, c denotes the sound speed and the normal velocity $v_n = \mathbf{v}.\mathbf{n}$ on the exterior surface S of the track radiating into the fluid is taken as a boundary condition of the 3D problem.

2.2.2 Wave-number domain

In the wave-number domain, the Helmholtz equation reduces to a set of 2D equations in the plane of the track section. For each wave-number κ, the spatial Fourier transform of the pressure $\tilde{p}(\kappa, y, z) = \int_{-\infty}^{+\infty} p(x, y, z)e^{-j\kappa x}dx$ verifies:

$$\Delta_{2D}\tilde{p} + (k^2 - \kappa^2)\tilde{p} = 0$$
$$\text{with} \quad \frac{\partial \tilde{p}}{\partial \mathbf{n}} = j\omega\rho\tilde{v}_n \quad \text{on } \Gamma \tag{4}$$

where the boundary condition of the problem is here given by the normal velocity $\tilde{v}_n = \tilde{\mathbf{v}}.\mathbf{n}$ on the exterior perimeter Γ of the track section and where the effective acoustic wave-number depends on the structural wave-number. An important point is that wave-numbers κ such that $\kappa > k$ give rise to evanescent acoustic waves and can be neglected.

2.2.3 Radiated power

Furthermore, the total power radiated by the track can be determined by integration in the wave-number domain rather than by integration along the track length:

$$P = \frac{1}{2}\Re\left(\int_{-\infty}^{+\infty}\int_{\Gamma} p^*(x, y, z)v_n(x, y, z)d\Gamma dx\right)$$
$$= \frac{1}{2\pi}\int_{-k}^{+k}\frac{1}{2}\Re\left(\int_{\Gamma}\tilde{p}^*(\kappa, y, z)\tilde{v}_n(\kappa, y, z)d\Gamma\right)d\kappa$$
$$= \frac{1}{\pi}\int_{0}^{+k}\tilde{P}(\kappa)d\kappa \tag{5}$$

where $\tilde{P}(\kappa)$ is the power radiated by the track at wave-number κ for the 2D transformed problem (cf. Eqn. (4)).

2.3 Numerical implementation

The numerical implementation of the formulation can be achieved simply using a calculation software dedicated to 2D exterior acoustic problems. The process described below must be performed for each considered pulsation ω.

2.3.1 Vibrations on the track perimeter

The first step consists in extracting a mesh of the perimeter of the track section and then determining the vector $\mathbf{V_i}$ of velocities corresponding to the magnitudes of the different waves $\mathbf{v_i}(\mathbf{y}, \mathbf{z})$ at the degrees of freedom of the mesh, resulting from the considered excitation.

2.3.2 Fourier transform

In a second step, the vectors $\mathbf{V_i}$ are to be expressed in the discretized wave-number domain according to Eqn. (2):

$$\tilde{\mathbf{V}}_{\mathbf{q}} = \tilde{\mathbf{V}}(\kappa_q) = \sum_{i=1}^{N}\mathbf{V_i}\frac{2j\hat{\kappa}_i}{\kappa_q^2 - \hat{\kappa}_i^2} \tag{6}$$

The choice of κ_q values for the discretization must be carefully made on the basis of the complex poles $\hat{\kappa}_i$. In particular, a fine step is recommended around the poles with low attenuation, i.e. with low imaginary parts, for which "resonance" may occur.

2.3.3 2D acoustic simulations

For each κ_q value, a 2D acoustic simulation is then launched from the $\tilde{\mathbf{V}}_q$ vector allowing the calculation of radiated acoustic power $\tilde{P}_q = \tilde{P}(\kappa_q)$. In order to use external acoustic software to solve the transformed 2D problem (cf. Eqn. (4)), the transformation of the acoustic wave-number is carried out indirectly by specifying a specific sound speed for each simulation:

$$c_q = \frac{\omega}{\sqrt{k^2 - \kappa_q^2}} \tag{7}$$

2.3.4 Summation of acoustic powers

Finally, the total radiated power is determined by integrating the power values corresponding to the different simulations according to Eqn. (5). A simple trapezoidal method is implemented:

$$P = \frac{1}{\pi}\sum_{q=1}^{N_q-1}(\kappa_{q+1} - \kappa_q)\left(\tilde{P}_q + \tilde{P}_{q+1}\right) \tag{8}$$

3. VALIDATION OF THE METHOD

Two comparisons are carrying out to validate the method. The calculation of the 2D sound radiation is performed using a commercial calculation software (Actran$^{\text{TM}}$) based on the acoustic finite element method (FE) combined with perfectly match layers (PML) for the treatment of the unbounded exterior domain.
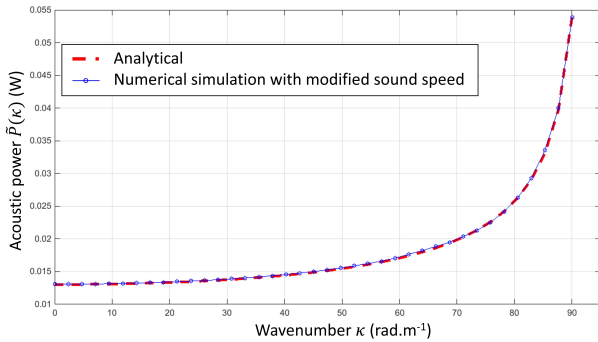
3.1 Sound radiated by a pulsating cylinder

First, the validation of the modification of the acoustic wave-number by means of the correction of the sound

10$^{\text{th}}$ Convention of the European Acoustics Association
Turin, Italy • 11$^{\text{th}}$ – 15$^{\text{th}}$ September 2023 • Politecnico di Torino
245

speed is achieved by considering the case of a radially oscillating cylinder of radius R, characterized by a radial velocity $v_r(x) = v_0 \exp^{-j\kappa x}$ on its surface. On the one hand, the sound power $\tilde{P}(\kappa)$ radiated by the cylinder can be obtained analytically [6]:

$$\tilde{P}(\kappa) = \frac{\pi R \rho \omega v_0^2}{k_r \Re(j H_0^{(1)}(k_r R))} \qquad (9)$$

where $k_r = \sqrt{k^2 - \kappa^2}$ and $H_0^{(1)}(\cdot)$ represents the Hankel function of the first kind and order 0. On the other hand, the radiated sound power is determined with the help of 2D numerical simulations with $\tilde{v}_r = v_0, \forall \kappa$ on the perimeter of the cylinder section and correction of the sound speed according to Eqn. (7).

Fig. 1 shows the results obtained at 5000 Hz. The two curves are very close. It can also be noted that the sound power tends to infinity for large structural wave-numbers κ approaching the acoustic wave-number $k = 92.4$ rad/m, which might cause some problems for the integration stage. However, this is due to the vibration magnitude $\tilde{v}_r$, which is here imposed constant for all wave-numbers. This is not the case for the specific vibration fields given in Eqn. (2).


Figure 1. Comparison between sound powers $\tilde{P}(\kappa)$ obtained analytically and computed with the proposed numerical method for a pulsating cylinder at 5000 Hz

3.2 Sound radiated by an open rail

The second validation is carried out on the basis of the track model proposed by Nilsson *et al* [2]. The track is composed of a 40E1 light rail laying on a very soft rail-pad. The authors propose a method very similar to the one presented in this paper but with an in-house implementation of the boundary element method (BEM) for computing the rail sound radiation in the wave-number domain. The BEM is modified directly to take into account the change in acoustic wave-number. All the details are given in reference [2]. The rail is not baffled in this simulation.
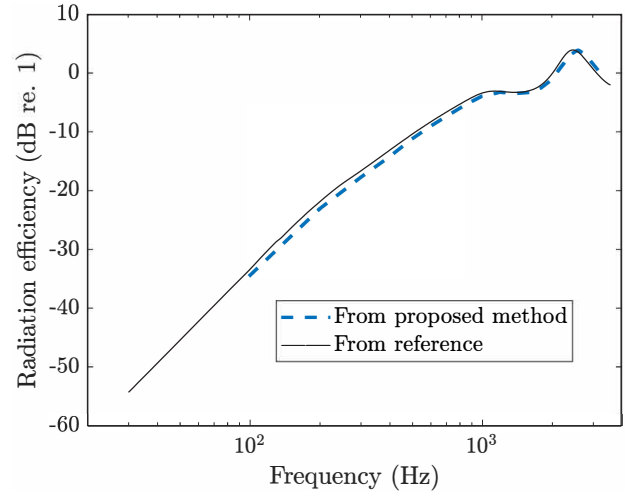
Figure 2. Comparison between radiation efficiencies σ given in reference [2] and obtained with the proposed implementation

Fig. 2 shows the comparison between the sound radiation efficiency given in [2] and obtained with the proposed method, e.g. based on the FE/PML method implemented in an external commercial software. As a reminder, the radiation efficiency is determined from the sound radiated power and the normal vibration velocity integrated on the radiating surface of the track:

$$\sigma = \frac{P}{\frac{1}{2}\rho c \int_{-\infty}^{+\infty} \int_{\Gamma} |v_n|^2 d\Gamma dx} \qquad (10)$$

Both methods give very similar and expected results. The open un-baffled rail behaves like a dipole (with a variation in $30 \log \frac{f}{f_0}$) before the critical frequency f_0 and exhibits interference effects related to its geometry at higher frequencies causing oscillations in the radiation efficiency [2, 4].

4. APPLICATION TO TRAM TRACKS

The proposed method is then used to study the sound radiated by two tram tracks.

4.1 Description of the track models

The first track is a classic ballasted track composed of a 50E6 Vignole rail, laying on a mono-block concrete sleeper by means of a rail-pad of medium stiffness. Fig. 3 shows the developed FE model for this track. Supporting components are modeled through elastic layers in the model. Low density values are chosen for the ballast and the rail-pad whereas a high Young modulus is chosen for the assumed rigid sleeper. Other structural parameters, including sleeper density, pad and ballast Young moduli as well as damping factors, have been updated on the basis of vibration measurement performed on an existing tram track (cf. track D in reference [7]). For the acoustic computation, the rail is baffled at foot level with an uniform impedance condition varying with frequency. The impedance value is determined by means of a Delany-Bazley model [8] assuming an air flow resistivity of 50×10^3 Pa.s.m^{-1} for the ballast.
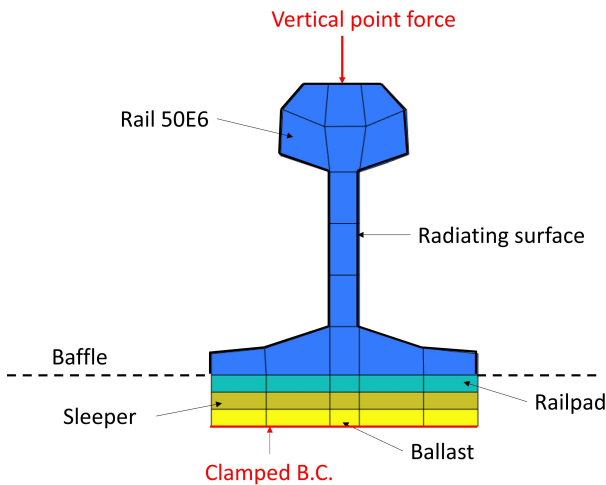
Figure 3. Model for the ballasted tram track with open rail

The second track is a slab track composed of a 41GPU grooved rail laying on a mono-block concrete sleeper through a soft rail-pad. The rail is embedded in a thin layer of grassy soil above the slab through "fill" elastic materials (some kind of polyethylene foam) of rather low density. The sleeper itself is rigidly embedded in the concrete slab. Fig. 4 shows the developed FE model for this track. The slab and the sleeper are assumed to be rigid whereas the mechanical effect of the grass cover is par-

tially neglected: only the low part of the fill elastic material is considered as solidly fixed by the soil. Low density value is chosen for the elastic layer representing the rail-pad. Other structural parameters, including fill material density and damping factors, have been updated on the basis of vibration measurement performed on an existing tram track (cf. track B in reference [7]). For the acoustic computation, the rail is baffled at the edge of the rail running surface with an uniform impedance condition also determined by a Delany-Bazley model but with an air flow resistivity of 200×10^3 Pa.s.m^{-1} for the grass cover.
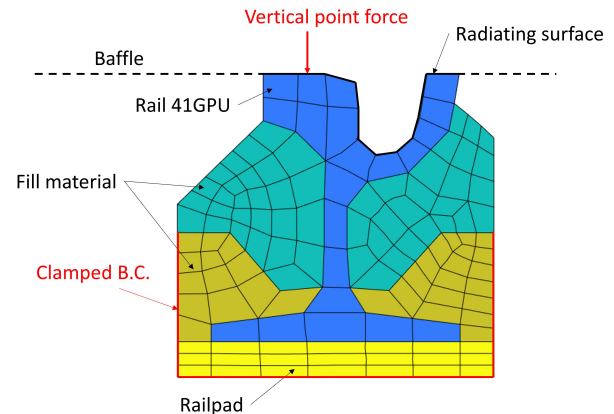
Figure 4. Model for the slab tram track with embedded rail

4.2 Vibration results

Wave shapes and wave-numbers have been determined for both tracks in the range $100 - 5000$ Hz by means of the wave-guide finite element method proposed in [2]. The results are briefly presented for a vertical point force $\delta(x)f(y_0, z_0)$ applied on the rail-head (cf. Fig. 3 and Fig. 4) in terms of point mobility and track decay rate.

4.2.1 Point mobility

Fig. 5 shows the variation of the magnitude of the vertical point mobility $Y_{zz} = v_z(0, y_0, z_0)/f(y_0, z_0)$ with frequency for both tracks.

For the ballasted track, three peaks are observed. The two resonances below 1000 Hz are caused by the beam-like vertical bending wave of the rail. Around 200 Hz, the sleeper/rail mass oscillates on the ballast stiffness while around 700 Hz, the rail mass oscillates on the rail-pad
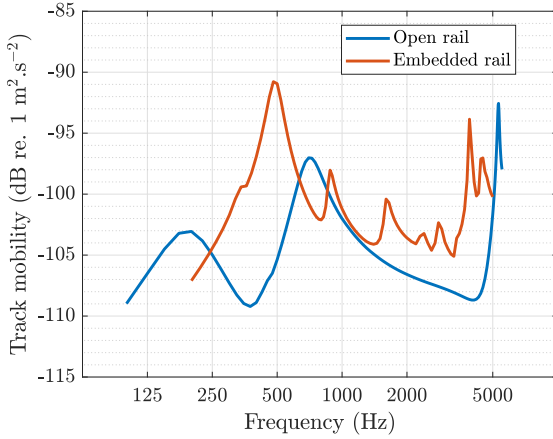
Figure 5. Magnitude of the vertical point mobility Y_{zz} as a function of frequency for both tracks

stiffness. The "resonance" located around 5000 Hz involves waves with deformation of the rail section, mainly web bending.

Generally speaking, the slab track with embedded rail is more flexible than the ballasted track. A pronounced rail/rail-pad resonance can also be observed but around 500 Hz. Due to the specific rail geometry and the location of the excitation, other peaks can be observed between 500 and 3000 Hz which are mainly related to beam-like waves characterized by coupled movements of torsion and lateral bending of the rail. Unlike the case of the ballasted track, these waves contribute significantly to the vertical response. At higher frequencies, several resonances involving waves with deformation of the rail section can also been observed.

4.2.2 Track decay rate

The structural models have also been use to determine the vertical track decay rate (TDR) for both tracks. The track decay rate quantifies the mean attenuation of the vibration level along the rail. In the case of a single wave, it can be easily determined from the complex wave-number $\hat{\kappa}_i$ by TDR$= 20\log(e)\hat{\kappa}_i$. However, in the general case, an "experimental" TDR has to be calculated, according to the following standard definition [9]:

$$\text{TDR} = \frac{4.343}{\sum_{n=1}^{n_{\max}} \frac{|v_z(x_n,y_0,z_0)|^2}{|v_z(0,y_0,z_0)|^2}(x_{n+1}-x_n)} \quad (11)$$

where the abscissa x_n are also defined in [9]. Fig. 6 shows the variation of the TDR with frequency for both tracks.
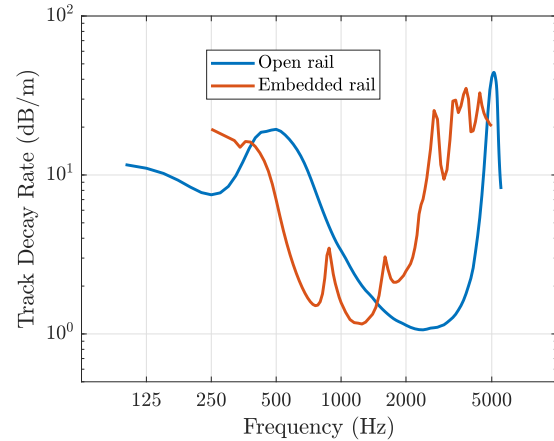
**Figure 6**. Track decay rate (TDR) as a function of frequency for both tracks

Similar variation can be observed for both tracks but with a shift to the low frequencies for the slab track with embedded rail due to the higher flexibility of the support. Rather low track rates ($<$ 3 dB/m) are found between 1000 et 4000 Hz for the ballasted track versus 600 and 2000 Hz for the slab track. Indeed, in these ranges, the attenuation values of the main contributing waves (vertical bending for the open rail versus vertical bending and torsion/lateral bending for the embedded rail) are also quite low with the same order of magnitude.

4.3 Acoustic results

The sound power radiated by the two tracks and the corresponding radiation efficiencies have been determined using the proposed numerical method in the range $100 - 5000$ Hz. In the context of a rolling noise application, it seems more appropriate to compare different tracks for a unit velocity excitation rather than a unit force (cf ref. [2]). Therefore, a normalized power is determined as follows:

$$P_v = \frac{P}{|v(0,y_0,z_0)|^2} \quad (12)$$

A first look to the radiation efficiencies (cf. Fig. 7) shows very different behaviors for the two tracks. For the open rail, the results compares well with those obtained in ref. [2] for an un-baffled open rail (cf. Fig. 2), excepted that the dipole-like behavior is no more found
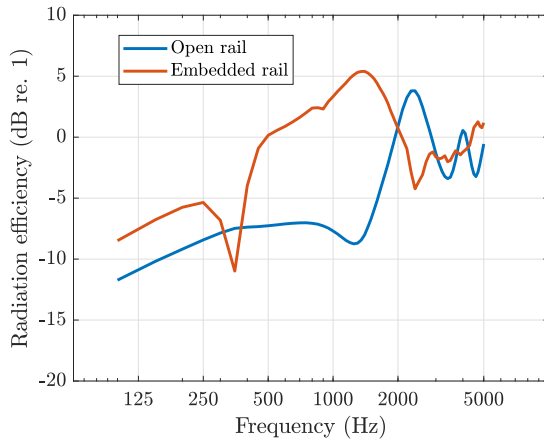
Figure 7. Radiation efficiency σ as a function of frequency for both tracks

below 1000 Hz due to the pronounced effect of the baffle. Above 2000 Hz, the radiation efficiency oscillates around unity (0 dB), due interference phenomena. In contrast, the radiation efficiency of the embedded rail reaches unity at much lower frequencies (500 Hz), showing particularly high values between 500 and 1000 Hz. This is rather significant and need to be investigated. The combined influence of the specific rail geometry and the high contributions of the torsional/lateral bending waves are probably involved.
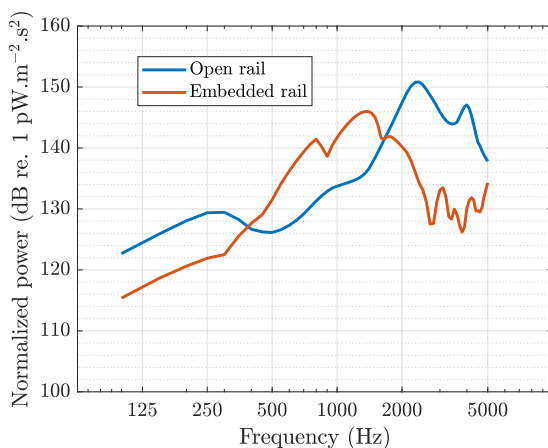
Figure 8. Normalized radiated sound power P_v as a function of frequency for both tracks

These observations are helpful to compare the results in terms of normalized radiated sound power (cf. Fig. 8). At frequencies above 2000 Hz, the normalized sound power radiated by the embedded rail is largely lower than the power radiated by the open rail. Since the radiation efficiencies of both rail are rather similar in this range, the difference may be explained by (i) a lower radiating perimeter and (ii) a lower average squared velocity, due to a higher track decay rate. At frequencies below 400 Hz, the normalized sound power radiated by the embedded rail is slightly lower than the power radiated by the open rail. The same previous factors (i) and (ii) may explain the difference but the effects are partially compensated by the higher radiation efficiency of the embedded rail in this range. At frequency between 500 and 2000 Hz, the normalized sound power radiated by the embedded rail is largely higher than the power radiated by the open rail. It may be explained on the one hand by a larger radiation efficiency and on the other hand by a lower track decay rate. The lower radiating perimeter of the embedded rail only partially compensates for these effects. This is an important result since the contribution of the rail sound radiation to rolling noise is major in this range.

5. CONCLUSION

Modeling of the noise radiated by railway tracks is necessary to estimate the rolling noise emitted by railway vehicles in detail and to propose effective means of reduction. In this perspective, the study of the sound radiated by tram tracks has been little studied. In particular, the limitations of 2D models are not well known and it is necessary to perform 3D simulations. In this paper a method is proposed to obtain 3D results by combining 2D simulations with the help of a wave-number decomposition. In particular, it is shown how the use of commercial acoustic software can be used for this purpose. The first results obtained on tram tracks show interesting phenomena, in particular that embedded rails can generate more noise than open rails in some frequency bands. Although these results need further investigation, they show the potential of the proposed method.

6. ACKNOWLEDGMENT

7. REFERENCES

[1] D. J. Thompson, *Railway Noise and Vibration: Mechanisms, Modelling and Means of Control*. Elsevier, 2009.

[2] C. M. Nilsson, C. J. C. Jones, D. J. Thompson, and J. Ryue, "A waveguide finite element and boundary element approach to calculating the sound radiated by railway and tram rails," *Journal of Sound and Vibration*, vol. 321, pp. 813–836, 2009.

[3] W. Li, R. A. Dwight, and T. Zhang, "On the study of vibration of a supported railway rail using the semi-analytical finite element method," *Journal of Sound and Vibration*, vol. 345, pp. 121–145, 2015.

[4] D. J. Thompson, C. J. C. Jones, and N. Turner, "Investigation into the validity of two-dimensional models for sound radiation from waves in rails," *The Journal of the Acoustical Society of America*, vol. 113, pp. 1965–1974, 2003.

[5] D. J. Thompson, G. Kouroussis, and E. Ntotsios, "Modelling, simulation and evaluation of ground vibration caused by rail vehicles," *Vehicle System Dynamics*, vol. 57(7), pp. 936–983, 2019.

[6] A. Pierce, "Basic Linear Acoustics," in *Springer Handbook of Acoustics* (T. Rossing, ed.), Springer Handbooks, pp. 25–111, New York, NY: Springer, 2007.

[7] O. Chiello, A. Le Bellec, M.-A. Pallas, P. Muñoz, and V. Janillon, "Characterisation of wheel/rail roughness and track decay rates on a tram network," in *Proceeding of the 48th International Congress and Exposition on Noise Control Engineering (Inter-Noise 2019)*, (Madrid, Spain), pp. 5024–5033, 2019.

[8] M. E. Delany and E. N. Bazley, "Acoustical properties of fibrous absorbent materials," *Applied Acoustics*, vol. 3, pp. 105–116, 1970.

[9] European standard EN 15461+A1. "Railway applications - Noise emission - Characterisation of the dynamic properties of track sections for pass by noise measurements."